energyequipsys/ Vol 2/No2/AUG 2014/ 141-154

ENERGY EQUIPSYS

Energy Equipment and Systems

http://energyequipsys.ut.ac.ir
http://energyequipsys.com

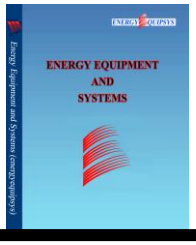

Improvement of thermal performance of a solar chimney based on a passive solar heating system with phase-change materials

Mohammad Safari [a]
Farschad Torabi [a]*

[a] School of Mechanical Engineering, K. N. Toosi University of Technology, Tehran, Iran

Article history:

Received 17 July 2014
Accepted 14 September 2014

ABSTRACT

Passive solar systems such as solar chimneys need solar radiation in order to work. Therefore, they cannot present stable natural ventilation when solar energy vanishes: to have a more robust and stable condition, solar energy should be stored during the day and released back during the night. Phase change materials can save additional thermal energy during the day and release it during the night in order to facilitate stable ventilation. In this study, a CFD simulation has been performed to investigate the effect of phase-change materials (PCM) utilization in the solar chimney to provide a stable temperature and air flow rate for a guardroom. The simulation was carried out for a whole day in winter in two cases: with and without PCM usage. The results show that use of PCM as an energy storage device significantly enhances the temperature stability of the guardroom.

Keywords: Passive Heating; Solar Chimney; Phase Change Materials (PCM); CFD Simulation; Parallel Computing.

1. Introduction

One of the major energy consuming sectors is buildings. According to the reports of the Department of Energy (DOE) of the United States, in most developed countries, buildings consume about 40% of the total energy used in that country. Therefore, any reduction in energy consumption in this sector decreases the total consumed energy. Normally, the energy used for heating and cooling comes from electricity, which is produced in power plants, most of which use fossil fuels. Consuming fossil fuels for power generation has two major drawbacks: firstly, the amounts of fossil fuels are limited and are going to finish in the near future, and secondly, they lead to environmental pollution. Therefore, there is a need to explore new alternative strategies and solutions to reduce human dependency on fossil fuels to provide amenities in buildings in upcoming years [1].

The heating and cooling process in buildings can be categorized into active and passive systems. Active systems consume more energy than passive ones because they use energy to derive their mechanical components, such as electrical motors or pumps. Moreover, in active systems, the use of complicated control systems, high-tech components and automatic dampers is unavoidable, and these are also energy-consuming components. This means that active systems depend indirectly on fossil fuels. On the other hand, passive methods work quietly without energy consumption. They therefore do not need fossil fuels either directly or indirectly, and they can decrease the heating and cooling sector of energy consuming buildings.

*Corresponding author:
School of Mechanical Engineering, K. N. Toosi University of Technology, Tehran, Iran.
E-mail address: ftorabi@kntu.ac.ir (Farshad Torabi)

Passive solar technologies can be placed into two categories: 1) passive solar heating and natural ventilation via a buoyancy effect; and 2) passive solar cooling via an evaporative effect. The well-known technologies that operate through a buoyancy effect for heating are the Trombe wall, solar chimney, unglazed transpired solar facade and solar roof [2]. Among these passive heating systems, solar chimneysare suitable systems for good heating and natural ventilation for buildings. A solar chimney is an inclined or vertical channel that, which absorbs solar radiation and traps its thermal energy. The temperature of the chimney absorber increases and heats the air in the channel. By increasing the air temperature, its density decreases and so it rises. The difference of the air density between the inlet and outlet causes natural convection. Thus the air with lower temperature enters the channel, becomes warmer, and exits. Solar chimneys have different configurations that can be classified into two groups: solar wall collector and solar roof collector [3, 4].

Due to the importance of solar chimneys, they have been studied in recent years. Gan [5] applied a glazed solar chimney for heat recovery in a naturally-ventilated building to investigate its effect on efficiency. This study concluded that installing heat pipes in the channel reduces the buoyancy effect, and for obtaining the air flow rate needed, it must be made of wind forces. Rodrigues et al. [6] developed a model by using the fully averaged equations of motion and energy, along with a k-ε turbulence model, to show turbulent natural convection in a vertical channel, where its wall heats asymmetrically. The results present temperature and velocity profiles at the exit part of the duct, which could be beneficial for the design of the system.

As solar radiation is not constant during a day, the passive solar ventilation is unstable. In order to have a reliable and stable ventilation system, it is necessary to conserve extra energy in the presence of the sun and release it in its absence. Energy storage devices make this feasible; in fact, these devices are a strategy for correcting the discrepancy between the demand and supply of energy. They improve the performance and reliability of solar energy systems. There are some different energy storage methods: mechanical, electrical, thermal and thermochemical. Thermal energy storage happens as a change in the internal energy of materials as sensible or latent heat, or as a combination of both. As latent heat provides constant temperature storage, it attracted much attention during the late 1970s and early 1980s. Research on latent heat storage continues, and it has been considered in waste heat recovery, building energy conservation and air conditioning applications. The example of the latent heat storage materials are phase change materials (PCM). In PCM, storage occurs through their change of state from solid to liquid, or liquid to solid. They store 5-14 times more heat per volume than sensible heat materials such as water or rock [7]. Therefore, it is practical to utilize PCM in order for them to conserve extra energy and use it at time of thermal energy shortage in passive solar systems.

Liu et al. [8] investigated the thermal performance of a solar chimney with PCM heat storage. The experiment was performed with three heat fluxes of 500, 600 and 700 Wm^{-2}. The results exhibited that the fluctuations of the absorber surface temperature were the same during the phase change transition period for the three cases. The flow rate and average temperature of the air changed by absorber surface temperature variations. The maximum flow rate occurred in the case of 700 Wm^{-2} and the maximum average temperature of the air was demonstrated by 500 Wm^{-2}. The investigation concluded that at the early ventilation period, the maximum thermal efficiency was around 80% for three heat fluxes.

As is evident, many investigations have been performed to show the effect of passive solar methods for natural ventilation. Substantial numbers of them have studied the solar chimney. Amongst them, the PCM-based solar chimney [8] has also been considered to solve some of the problems of the solar chimney. Investigations on a combination of the PCM and solar chimney for natural ventilation have been carried out to exhibit the effect of PCM on solar chimney performance. In previous studies, the PCM-based solar chimneys were considered alone and were not connected to a specific heating area. This paper presents an integration of the PCM-based solar chimney with a guardroom. The objective of the present work is to find the effect of the application of the PCM in the solar chimney to provide a stable temperature and air flow rate during day and night for the guardroom. To achieve this, a guardroom of specific dimensions is equipped with a solar

chimney. Then the temperature of the room is calculated using a transient finite volume method considering the effect of natural ventilation. The simulation is carried out on a selected day in December with and without the use of PCM. Finally the results of the two different methods are compared. All the calculations are carried out with ANSYS Fluent software. The solar radiation is obtained by solving an equation and introduced to the software with a special user-defined function (UDF).

List of symbols

A_{mush}	*mushy zone constant* $(10^4 \sim 10^7)$
C_p	*Specific heat of capacity*, J kg^{-1} K^{-1}
C_1	*Inertial resistance factor*
E	*Total energy*, kg m^2s^{-2}
G_{sc}	*Solar constant*
H	*Total specific enthalpy*, J kg^{-1}
h	*Specific enthalpy of sensible heat*, J kg^{-1}
ΔH	*Specific enthalpy of latent heat*, J kg^{-1}
I_T	*Hourly solar radiation*, W m^{-2}
I_b	Beam radiation, W m^{-2}
I_d	Diffuse radiation, W m^{-2}
I_o	*Extraterrestrial radiation*, W m^{-2}
j_j	*diffusion flux of species J*
K	Conductivity coefficient, W $m^{-1}K^{-1}$
k_{eff}	Effective conductivity, W $m^{-1}K^{-1}$
K_t	*Clearness index*
L_F	*Liquid fraction*
L	*Latent heat of the material, J*
n	*the day number*
p	*Pressure*, kg $m^{-1}s^{-2}$
P	*Precipitation, mm*
R_b	*The ratio of beam radiation on inclined to horizontal surface*
R	*Percentage of relative humidity*
S_h	*Enthalpy source term*, J kg^{-1}
S	*Fraction of sunshine hours*
S_i	Porous media momentum term
T	*Temperature*
$T_{liquidus}$	Melting Temperature
$T_{solidus}$	Solidification Temperature
t	*Time, s*
u, v	$x-direction, y-direction$ *Velocity*, m s^{-1}
$\vec{v}$	*velocity vector*

Greek letters

α	*Permeability*, m^2
β_0	Thermal expansion coefficient
β	*The angle between the plane of the tilted surface and the horizontal* surface
γ	*azimut angle*
δ	Declination angle
ε	*small number* (0.001) *to prevent division by zero*
θ	*Incidence angle*
θ_z	*Zenith angle*
μ	*Dynamic viscosity*, kg $m^{-1}s^{-1}$
ρ_g	*Ground − reflected radiation*
ρ	*Density*, kg m^{-3}
τ_{eff}	*effective stress tensor matrix*, kg $m^{-1}s^{-2}$
φ	*Latitude of the location*
ω	*The hour angle*

Subscripts

ref	*Reference*

2.System Modelling and Mathematical Formulation

A guardroom in Tehran, Iran, was considered in this paper. The PCM-based solar chimney was integrated on the south side of the room as shown in Fig.1. The guardroom height and length was 2.5 m and 4 m, respectively. The top surface of the guardroom, the outer surface of the air channel (solar chimney), the outer surface of collector glass cover, and the collector absorber boundary conditions of the solution domain were a mix of solar radiation and convection. The outer surface of the walls, the outer surface of the air channel, which was on the side of the wall, and the bottom surface and edge of the collector boundary, had convection conditions. The bottom surface of the guardroom and the solar chimney boundary conditions were insulated. Some UDFs in ANSYS Fluent were used to compute the solar radiation, the heat absorbed by absorber, and the heat transfer by the outer surfaces via convection.

The roof consisted of three layers from top to bottom: tar-layer, brick, and stucco. The inner and outer surfaces of the walls were stucco and brick, respectively. The bottom of the collector consisted of three insulation layers: from outside to inside these were

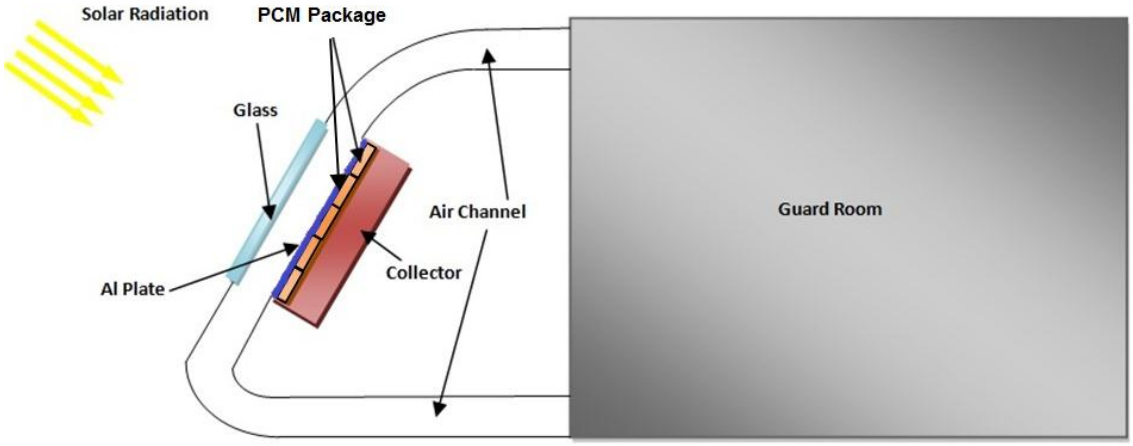

Fig. 1. The schematic of the integration of the PCM based solar chimney and the guard room

plywood, glass wool, and polystyrene. Other collector modules were a glass cover (transmissivity value of 0.9), an aluminium (Al) absorber (absorptivity value of 0.94), and a PCM layer of 25 cm thickness (sodium sulphate decahydrate $Na_2SO_4.10H_2O$; melting point 307 K, freezing point 303 K, and latent heat fusion 126 kJ kg^{-1}) for latent heat storage.

The PCM were placed in small rectangular packages behind the Al plate. In these packages, the PCM were not able to move along the collector after melting. Hence, PCM velocity after fusion was low and did not have a substantial impact on heat transfer. The fluid's movement was therefore ignored.

For simulation of the proposed design, special attention should be paid to the physical phenomena involved. More specifically, natural convection and phase changes are the most important phenomena in the present study. Although solar radiation is the core of passive heating systems, for simulation it renders itself only into boundary conditions. It should be noted that when PCM are being melted, it flows into its own designated space. The velocity magnitude of the melted PCM is about 10^{-5} ms^{-1}, which is almost zero, but the simulation shows that even that amount of movement may result in numerical instability. Since the induced velocity does not contribute to the heat transfer mechanism, which is the concept of the present study, it was assumed that PCM are confined in a porous matrix, which renders the movement of the melted PCM. This is simply a numerical technique for rendering the velocity of PCM, and it improves the stability of the solver.

According to the abovementioned physical phenomena, the governing equations should be written in a form that can predict the natural convection, phase change and porous media as follows:

1. Conservation of mass or continuity equation:

$$\frac{\partial \rho}{\partial t} + \nabla.(\rho \vec{v}) = 0 \qquad (1)$$

where ρ is the density of fluid and $\vec{v}$ is the velocity vector.

2. Conservation of momentum

For the present study, conservation of momentum takes the form[9]:

$$\frac{\partial(\rho \vec{v})}{\partial t} + \nabla.(\rho \vec{v}\vec{v}) = -\nabla P + \nabla.(M\nabla \vec{v}) + \frac{(1-L_F)^2}{L_F^{\,3}+\varepsilon} A_{mush}\vec{v} + \frac{\vec{g}\rho_{ref}(1-\beta_0(h-h_{ref}))}{C_p} + S_i \qquad (2)$$

where L_F, μ, A_{mush} and ε are, liquid fraction, dynamical viscosity, mushy zone constant (10^4~10^7), and small number (0.001) to prevent division by zero, respectively. Shear rates and heat generation were neglected.
The liquid fraction, L_F can be defined as:

$$L_F = \begin{cases} \dfrac{T - T_{solidus}}{T_{liquidus} - T_{solidus}}, & T_{solid} < T < T_{liquid} \\ 1, & T > T_{liquid} \\ 0, & T < T_{solid} \end{cases} \qquad (3)$$

The mentioned momentum equation consists of PCM melting phenomena by having the term $\frac{(1-L_F)^2}{L_F^{\,3}+\varepsilon} A_{mush}\vec{v}$ which is

eliminated for all materials except PCM in simulation because the liquid fraction was considered 1, as the solid and liquid temperatures were equal to, zero as per the ANSYS Fluent 14.5 settings.

Due to the small variation in temperature, Boussinesq approximation was used to consider natural convection. In this approach, density is constant in all equations except for the buoyancy force term in the momentum equation which varies with temperature as follows:

$$\rho = \rho_{ref}\left(1 - \beta_0\left(T - T_{ref}\right)\right) \quad (4)$$

In this equation ρ_{ref} and T_{ref} are the reference density and temperature respectively, and β_0 is the thermal expansion coefficient.

As mentioned and according to the low velocity of melted PCMs, PCM zones were considered as porous media with high viscosity and inertial loss terms. Porous media are modelled by the addition of a momentum source term to the standard fluid flow equations:

$$S_i = -\left(\frac{\mu}{\alpha} + \frac{C_1\rho}{2}|\vec{v}|\right)\vec{v} \quad (5)$$

where S_i is the source term for the i^{th} (x, y, or z) momentum equation, $|\vec{v}|$ is the magnitude of the velocity and α, and C_1 are the permeability and the inertial resistance factor respectively. It should be reemphasized that S_i is applied only in PCM zones.

3.Energy conservation

The balance of energy in the system takes the form:

$$\frac{\partial(\rho H)}{\partial t} + \nabla.(\rho\vec{v}H) = \frac{K}{C_p}\nabla^2 T \quad (6)$$

where H is the total enthalpy of the material. For the present application where a phase change occurs, the total enthalpy consists of both the sensible enthalpy, h, and the latent heat, ΔH; In other words we can write:

$$H = h + \Delta H \quad (7)$$

With this assumption, the energy equation covers all the involved thermal and heat transfer phenomena including phase change. Thus the equation is applicable to all the zones in the simulation. In phase change phenomena for PCM, the latent heat, ΔH, can be written in terms of the latent heat of the material, L in J as follows:

$$\Delta H = L_F.L \quad (8)$$

where L_F is the liquid fraction. So the latent heat can vary between zero (for a solid) and L (for a liquid). The sensible heat h also can be also obtained as follows:

$$h = mC_p(T_2 - T_1) \quad (9)$$

where m is the PCM mass Kg, C_p is Specific heat of capacity, $Jkg^{-1}K^{-1}$, and T_1, T_2 are the initial and final temperatures, respectively.

4.Simulation of solar radiation

For calculation of hourly radiation, some angles needed to be defined which are shown in Fig.2. The incidence angle, θ, the angle between the beam radiation on a tilted surface and the normal vector of that surface, is obtained from the equation [20]:

$$\begin{aligned}\cos\theta &= \sin\delta\sin\varphi\cos\beta \\ &\quad -\sin\delta\cos\varphi\sin\beta\cos\gamma \\ &\quad +\cos\delta\cos\varphi\cos\beta\cos\omega \\ &\quad +\cos\delta\sin\varphi\sin\beta\cos\gamma\cos\omega \\ &\quad +\cos\delta\sin\beta\sin\gamma\sin\omega\end{aligned} \quad (10)$$

The zenith angle θ_z the angle between the vertical line and the line to the sun is obtained from:

$$\begin{aligned}\cos\theta_Z &= \sin\delta\sin\varphi \\ &\quad +\cos\delta\cos\varphi\cos\omega\end{aligned} \quad (11)$$

In these equations, β is the angle between the plane of the tilted surface and the horizontal surface, φ is the latitude of the location and ω is the hour angle. The angular displacement of the sun from east or west due to rotation of the earth around its axis is 15^o per hour; therefore hour, angle, and local time are related to each other by the following equation:

$$\omega = (t - 12) \times 15 \quad (12)$$

The surface azimuth angle, γ, is the deviation of projected normal vector on the horizontal plane from the local meridian, with zero direction. The declination angle, δ, is the angular location north or south of the equator, as follows:

$$\delta = 23.45\sin\left(360\frac{n + 284}{365}\right) \quad (13)$$

where n is the day number starting from January 1^{st}.

To estimate the solar radiation received by

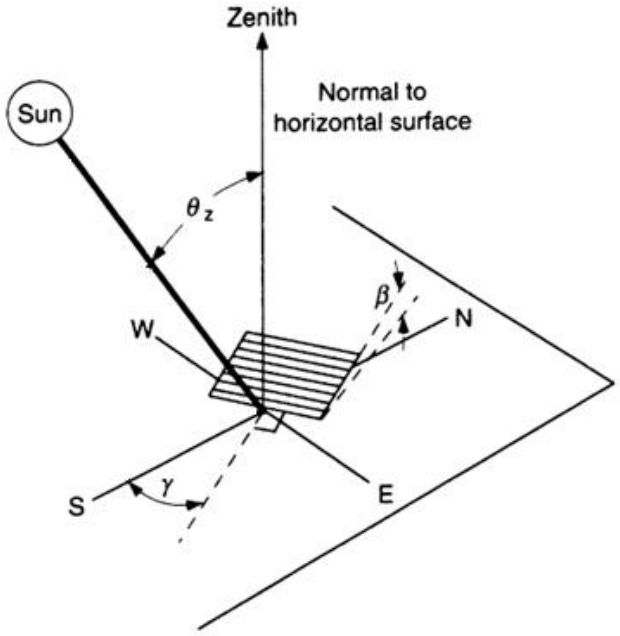

Fig. 2. Defined angles of solar radiation on a tilted surface [10].

the absorber surface- the roof surface and the outer surface of the solar chimney sloped surfaces- the isotropic diffuse mode can be used, which assumes a solar radiation consisting of three components: beam, isotropic diffuse, and solar radiation diffusely reflected from the ground. Diffusive radiation strongly depends on the clearness index of the atmosphere. Clearness index is a fraction of solar irradiation, which travels through the atmosphere and reaches the Earth's surface. This index is a function of atmospheric parameter, which can be written as:

$$K_T = f(T, R, P, S) \tag{14}$$

where T is atmospheric temperature, R is the percentage of relative humidity, P is precipitation and S is the fraction of sunshine hours. Obtaining this factor is crucial for any solar simulation and strongly varies from location to location. For the city of Tehran, Vehedi et al. [11] proposed the following relation:

$$K_T = 0.8417S + 0.02332T - 0.03184ST \tag{15}$$

Note that in this equation, T is expressed in degrees Celsius. Having K_T, the solar beam radiation at the panel surface, I, can be easily estimated as:

$$I = K_T . I_o \tag{16}$$

where I_o, the solar irradiation at the atmosphere edge, is defined as follows:

$$I_o = \frac{24 \times 3600}{2\pi} G_{sc} \left[1 + 0.033 \frac{360n}{365}\right] \times \left[\begin{array}{l}(cos\varphi cos\delta (sin\omega_2 - sin\omega_1)) \\ + \frac{2\pi(\omega_2 - \omega_1)}{360} sin\varphi sin\delta\end{array}\right] \tag{17}$$

in which G_{sc} is the solar constant, assumed to be equal to 1367 Wm^{-2}.

There are some correlations that try to relate the diffusive flux to solar beam radiation and clearness index. For example [10]:

$$I_d = \begin{cases} I(1 - 0.249K_T), & K_T < 0.35 \\ I(1.557 - 1.84K_T), & 0.35 < K_T < 0.75 \\ 0.177I, & 0.75 < K_T \end{cases} \tag{18}$$

where I_d is the diffusive flux, K_T is the clearness index related to geographic-atmospheric parameters [11].

It is necessary to define a factor R_b to determine the ratio of total radiation on the tilted surface to that on the horizontal surface, which is obtained as follows:

$$R_b = \frac{cos\,\theta}{cos\,\theta_z} \tag{19}$$

Therefore, the hourly solar radiation I_T is obtained as the sum of three terms from the follow equation:

$$I_T = I_b R_b + I_d\left(\frac{1+\cos\beta}{2}\right) + I\rho_g\left(\frac{1-\cos\beta}{2}\right) \quad (20)$$

where $I\rho_g$ is the reflected radiation from the surroundings of the surface.

3.Simulation

The geometry shown in Fig. 1 was modelled with Gambit software and, as shown in Fig. 3, a structured mesh was generated for simulation. Different mesh sizes were used in order to make the solution mesh independent, as presented in Fig.4. The average room temperature and the Al-plate temperature at noon are shown in Table 1. The table shows that a numerical simulation using 81,965 computational cells is sufficient to achieve a mesh-independent solution. In this figure, the solar panel is shown with more detail. A portion of the panel is also magnified to show the details of the generated mesh where the PCM packs are located. As can be seen, each PCM pack is separated from the others; hence melted PCM are not able to flow along the solar panel.

As the PCM zone was considered as a porous media with high viscous resistance, there would be no substantial velocity after simulation. In other words, in this method, natural convection was ignored and heat transfer in PCM was only via conduction. Viscous resistance was considered at 1^{10} and porous formulation was set to superficial velocity. Moreover, the UDF code was prepared in C language for parallel computing using a message passing interface (MPI) in ANSYS Fluent to speed up the calculations.

Regarding the initial conditions, the temperature was set to 275 K, and the magnitudes of both X and Y velocity vector were set to $0.0001 ms^{-1}$. All initial conditions were constant for all cases. To eliminate the effect of initial conditions, as discussed before, the calculation was performed for four actual days. Thus, in order to have accurate, trust worthy results, the contours of the fifth day of simulation were analysed.

The ANSYS Fluent CFD code employs the finite volume method. The first-order implicit scheme was used for transient formulation. The PRESTO, the second order upwind method was utilized for the discretization of pressure, momentum, and energy, respectively. The well-known SIMPLE algorithm was specified for pressure-velocity coupling.

4.Results and discussion

To investigate the effect of PCM usage in passive solar heating systems, the guardroom discussed above has been simulated with and without PCM packs on a selected day in winter (specifically December 5^{th}) when the ambient temperature reaches about five degrees Celsius and the solar radiation is almost at a minimum during the year. Therefore, the selected day can predict the worst case for the guardroom.

The simulation was carried out for 24 hours a day; however, since the heat transfer is a transient phenomenon, which depends on initial conditions of the room, imposing a proper initial condition for the simulation is crucial. To obtain a proper initial condition, we start from a uniform temperature for the whole system assembly and solve the transient governing equations for five successive days. Since energy equation (Eq. 6) has a parabolic nature, the solution modifies itself as the simulation time passes. Hence, after four days of simulation, a proper initial condition is obtained for simulation of the 5^{th} day. For both cases, namely without and with PCM packs, the same procedure has been taken into account.

Table 1. Mesh size effect on average room temperature and Al-plate temperature at noon

Mesh Size	Al Plate Temp.	Average Room Temp.
343332	120	16
81965	120	17
25287	117	14

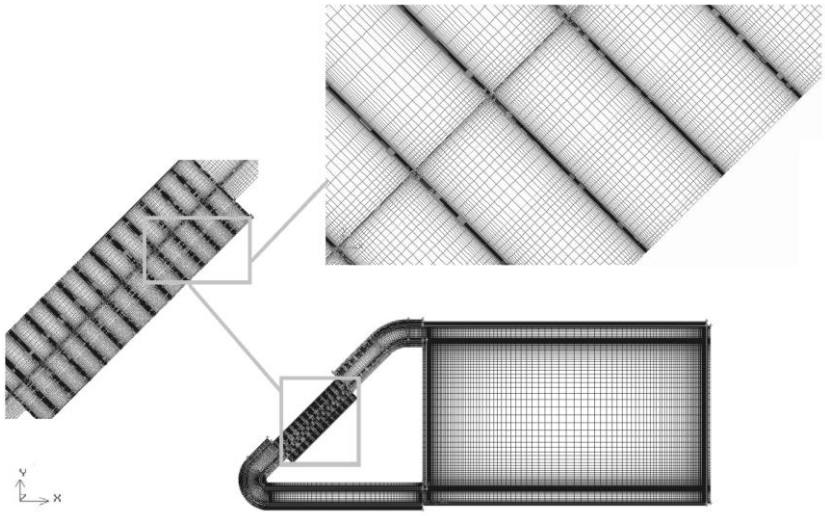

Fig. 3. Two-dimensional mesh (medium size) of the integration of the PCM based solar chimney with the guard room

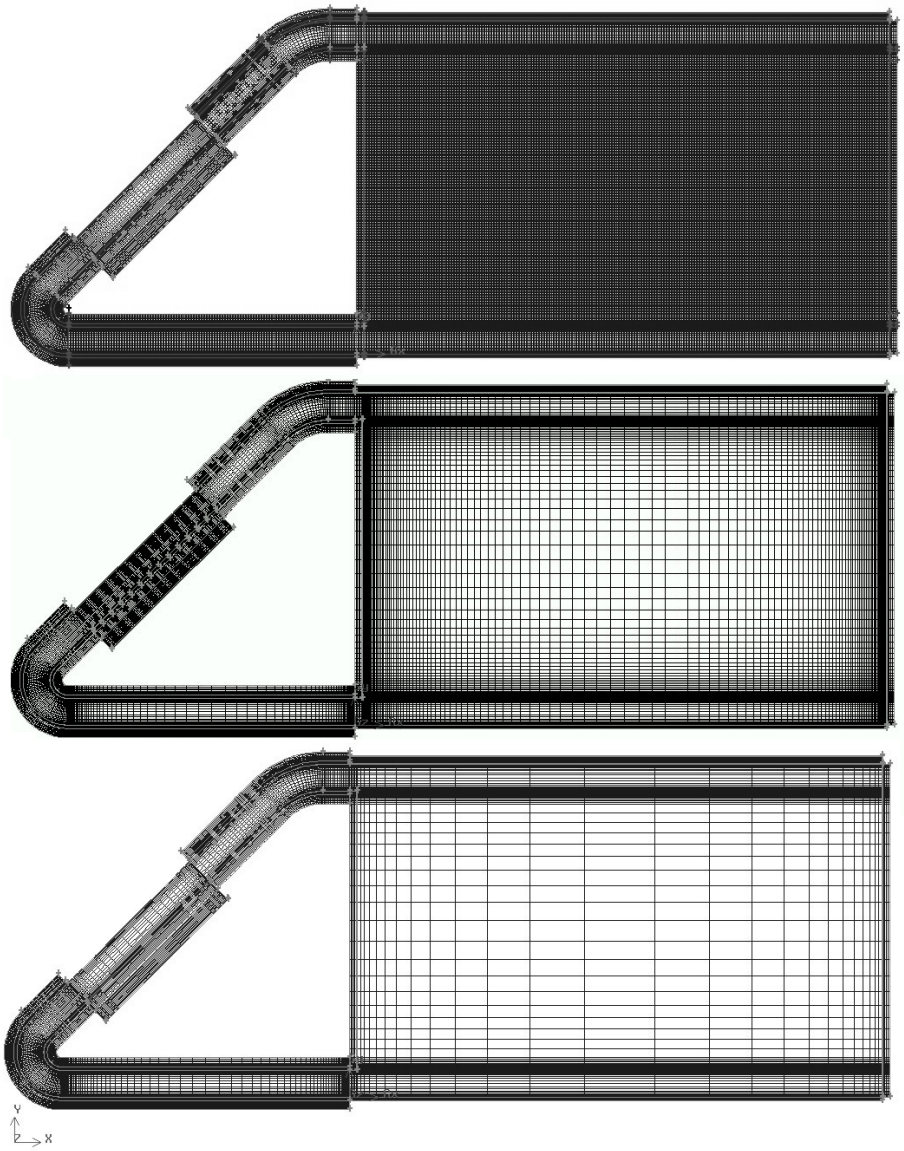

Fig. 4. Two-dimensional meshes in three different sizes

Figure 5 shows the solar radiation and ambient temperature during December 5th in Tehran. As we can see, and as expected, the solar radiation reaches its maximum level at around 12:00 PM, when the ambient temperature also reaches its maximum (around 12 degrees Celsius). Solar radiation can be captured by a solar thermal panel during the day to deliver the necessary thermal load to obtain a desired condition. However, during the night when the solar radiation disappears, the ambient temperature falls down to approximately five degrees Celsius. During this period of time, we cannot deliver the required heat load to the guardroom. Therefore, the temperature of the room falls below the design temperature.

Figure 6 presents a contour plot for guardroom temperature at 2:00 PM with no PCM packs installed in the solar panel. It is clear that the temperature of the room reaches around 19 degrees Celsius while the outside temperature is only 11 degrees Celsius. The temperature difference is due to the installation of a solar thermal panel and the designed solar chimney for air circulation.

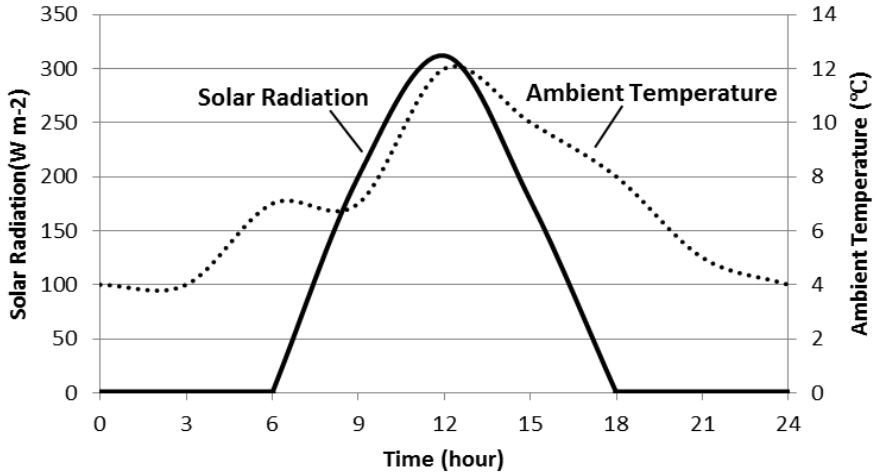

Fig. 5. Solar radiation and ambient temperature on December 5th in Tehran

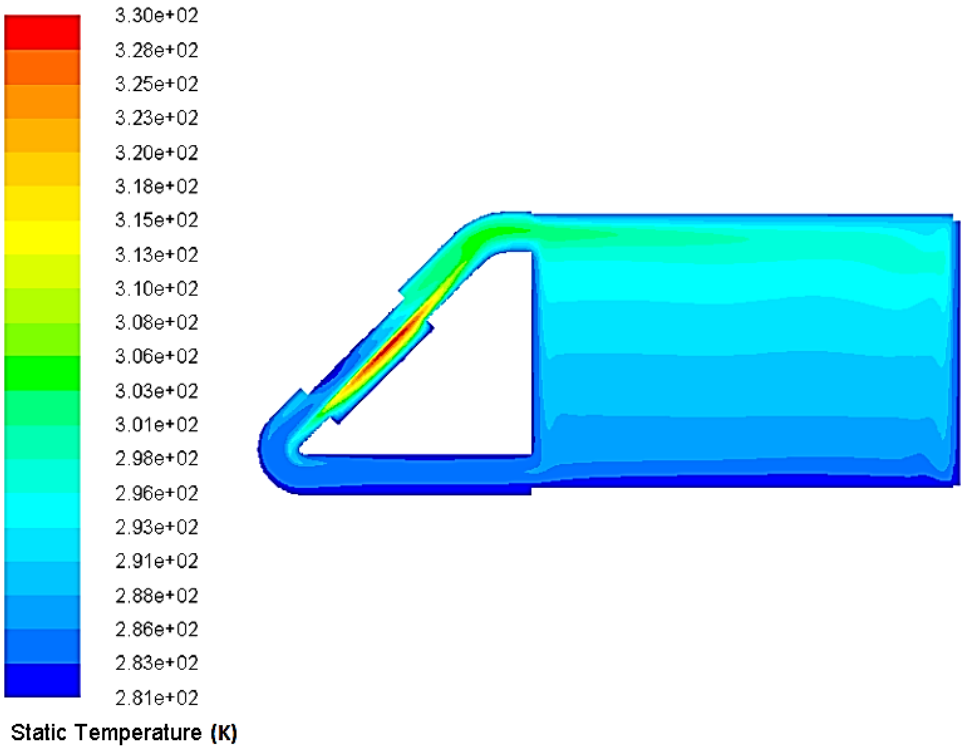

Fig.6. Contour plot for guardroom temperature at 2:00 PM without PCM

Figure 7 shows the vector plot at the same time inside the guardroom together with panel assembly. From the figure it is clear that the designed panel assembly (the solar panel and the solar chimney) induces natural convection inside the room. The highest speed of air circulation occurs at the solar panel area where the maximum temperature difference exists. The highest air velocity is about 2.52×10^{-2} ms^{-1}, which is not too much to disturb comfortable conditions; however, this velocity level plays an important role in heat transfer from the solar panel to the heating space. Natural circulation or convection causes the absorbed heat inside the solar panel be transferred to the guardroom.

Figure 8 shows the temperature contours in the room at 3:00 AM. As can be seen, although the guardroom is equipped with a solar panel, its temperature drops to around five degrees Celsius during the middle of the night. In other words, during the night the room temperature becomes equal to the ambient temperature, which is not desirable. This shows that a single solar panel, as discussed above, is unable to maintain the temperature of the room in the specified.

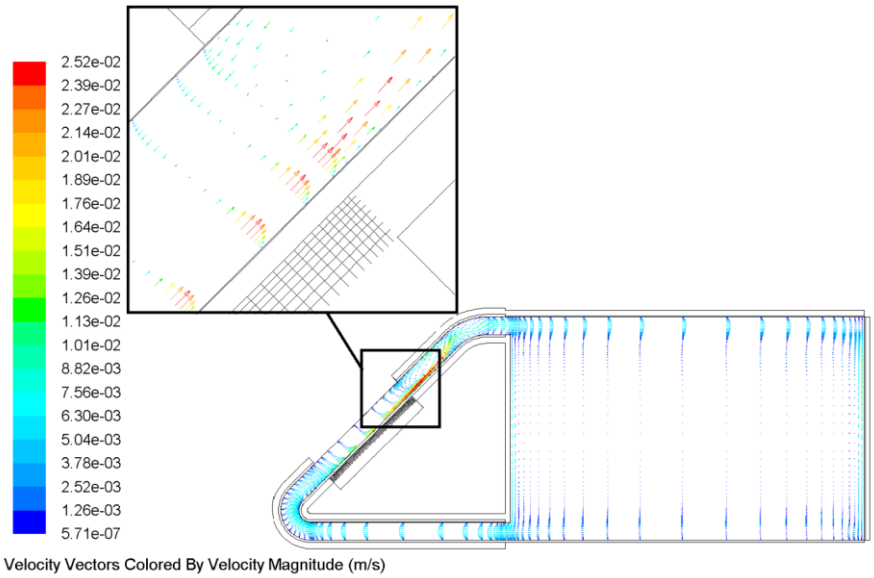

Fig. 7. Vector plot for guardrooms at 2:00 PM without PCM

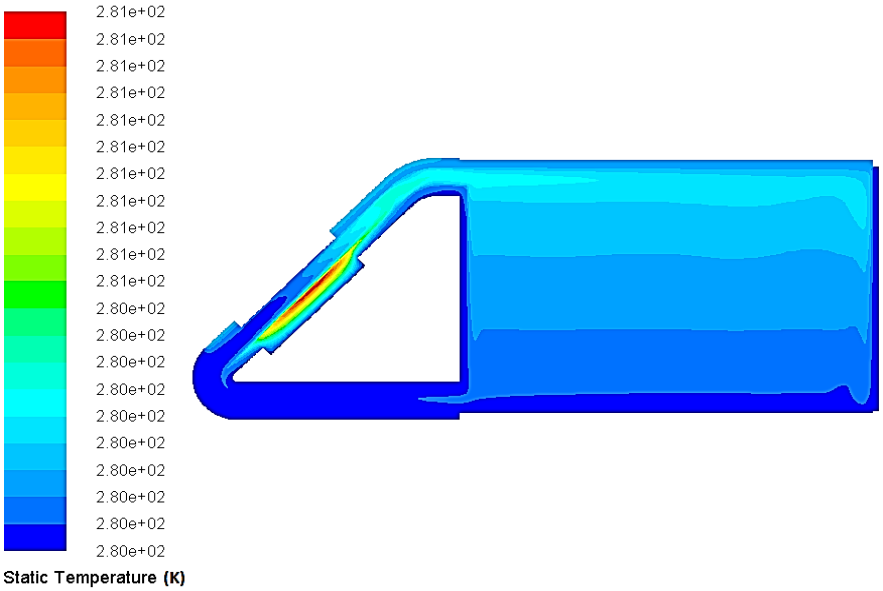

Fig. 8. Contour plot for guardroom's temperature at 3:00 AM without PCM

Until now, it has been shown that for good air conditioning, thermal solar heat should be stored in a storage device for space heating when there is no solar radiation. As discussed before, a good choice is to store thermal heat in PCM. To demonstrate the effect of energy storage on passive space heating, the same room is simulated once again, but at this time packets of PCM are placed inside the solar panel and the chimney walls. The rest of the figures deal with the results obtained from the simulation of the PCM-equipped panel.

Figure 9 shows the contours of a PCM liquid fraction at 3:00 AM and 1:00 PM. The blue colour means that the liquid fraction is zero, or, in other words, PCM are not melted yet and are in the solid state. The red colour, on the other hand, means that the liquid fraction is equal to one. This means that the PCM are melted and are in the liquid state. It should be noted that the colour inside the solar panel (the area above the PCM packets) is also shown as red, meaning that there is no solid material, or, in other words, this area is filled with a fluid air (not be confused with melted PCM).

As mentioned earlier in this paper, to obtain accurate initial conditions for simulation, we started from a uniform temperature at t=0 and marched in time for five days. What we see in Fig. 9 is the result of simulation on the fifth day. What is important here is the fact that the results shown in this figure are cyclic. This means that during the day, when solar energy enters the panel, it becomes warm and the PCM start melting. At 1:00 PM, as shown in the figure, all the PCM are melted. On the other hand, during the night, PCM release back the stored thermal energy and become solid again. For example at 3:00 AM, as we can see in figure, almost all the melted materials became solid again.

The process discussed above results in a uniform room temperature even in the absence of the sun. To check its performance, the temperature contours at 2:00 PM and 3:00 AM are shown if Figs. 10 and 11, respectively (these figures should be compared with Fig. 6 and 8). As we can see, with the usage of PCM, room temperature reaches around 15 degrees Celsius, which is less than the results obtained before (comparing Fig. 10 and 6). This means that the usage of PCM causes the peak of the room temperature to drop, because PCM absorb a portion of thermal energy gained by the solar panel to melt the PCM. However, at at 3:00 AM the room temperature becomes 12 degrees Celsius, which is much higher than earlier. This means that the PCM were able to sustain the room's temperature for a whole day. This is, in fact, the main purpose of the incorporation of the PCM into passive solar heating.

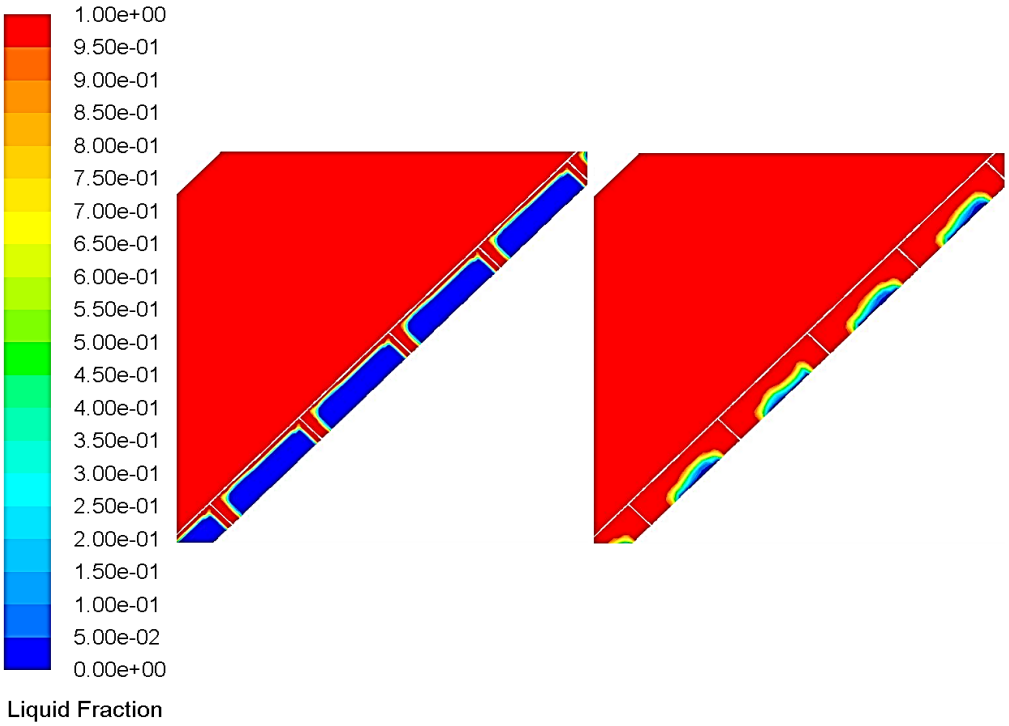

a) At 3:00 AM b) At 1:00 PM

Fig. 9. Contours of liquid fraction for PCM procedure (from a to b)

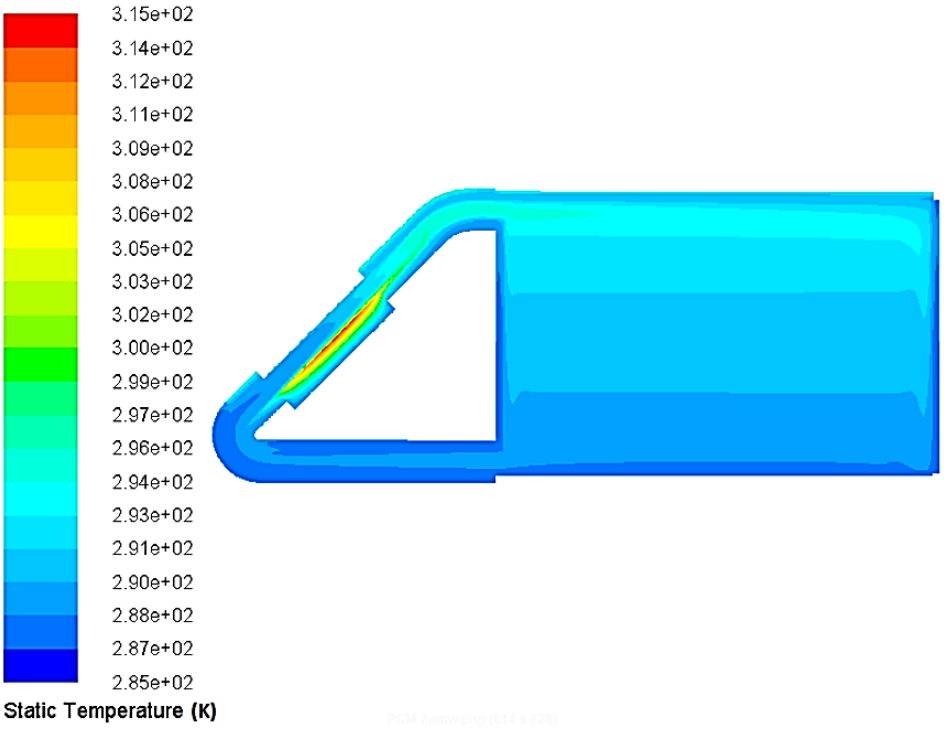

Fig. 10. Contour plot for guardroom temperature at 2:00 PM with PCM

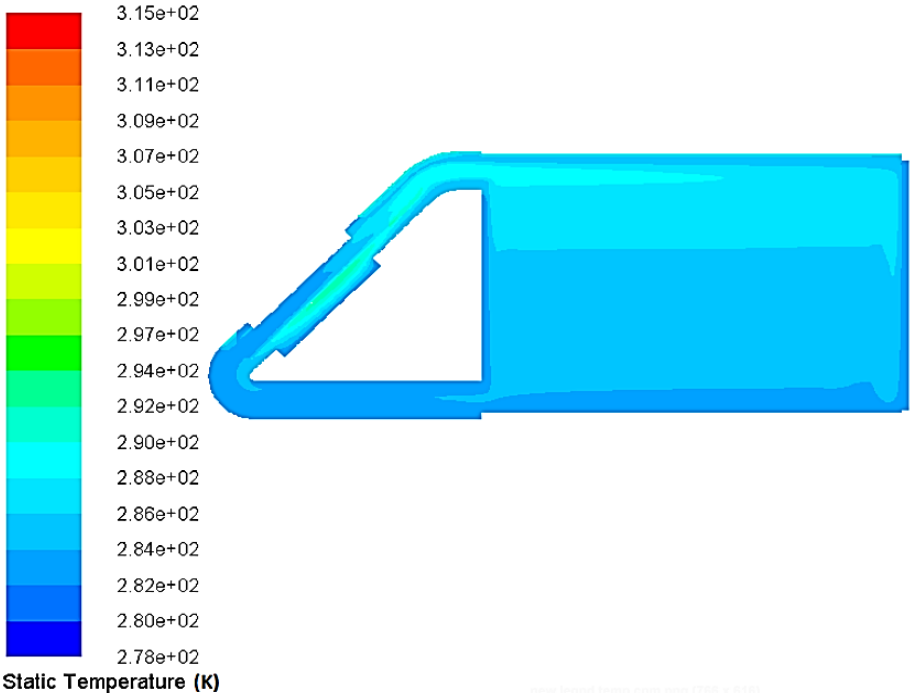

Fig. 11. Contour plot for guardroom temperature at 3:00 AM with PCM

To gain a better understanding of the whole simulation, the average temperature of the room for a whole day is plotted in Fig. 12, both with and without PCM. As is clearly seen in the figure, the usage of PCM results in a more uniform temperature during the day. On the other hand, PCM cause the peak temperature to decrease because they consume a part of the acquired solar energy.

From studying Fig.12, we notice that the variation in temperature across the 24 hours of the day is much higher when we do not use PCM in the solar collector. This fact reveals another drawback of this design, which is that thermal stress, is imposed on the solar panel. To develop a clearer understanding, Fig.13 shows the variation of the temperature of the solar panel body, which is made of aluminium. It is clear that the body material experiences a very high temperature gradient during the day, when there are no PCM inside the panel. More specifically, the base temperature reaches about 120 degrees Celsius during the peak solar radiation and about five degrees Celsius at night. However, PCM cause the base temperature to experience a much lower gradient. As can be seen in the figure, the temperatures of the panels equipped with PCM rarely exceed 70 degrees Celsius and do not reach lower than ten degrees Celsius. This fact is crucial for industrial sectors, where reliability is very important.

5.Conclusions

In the present work, the effect of the combination of solar thermal energy storage with solar passive heating was studied numerically. For energy storage, phase-changed materials were incorporated because the heat capacity is much greater during phase change. This enables one to design more compact energy storage for any purpose.

To show the effect of the PCM in solar passive cooling, a guardroom, which was equipped with a solar panel and chimney for air circulation and heating, was used. The integrated geometry was numerically analysed in two different cases; namely with and without the use of PCM. The results showed that by using PCM as a thermal energy storage system, the temperature of the guardroom can be maintained at an almost uniform levels for a whole day, while without the use of PCM, room temperature varies during day and night. Moreover, PCM cause the temperature of the solar panel to become more uniform and also reduce its peak temperature dramatically. This results into a more reliable system.

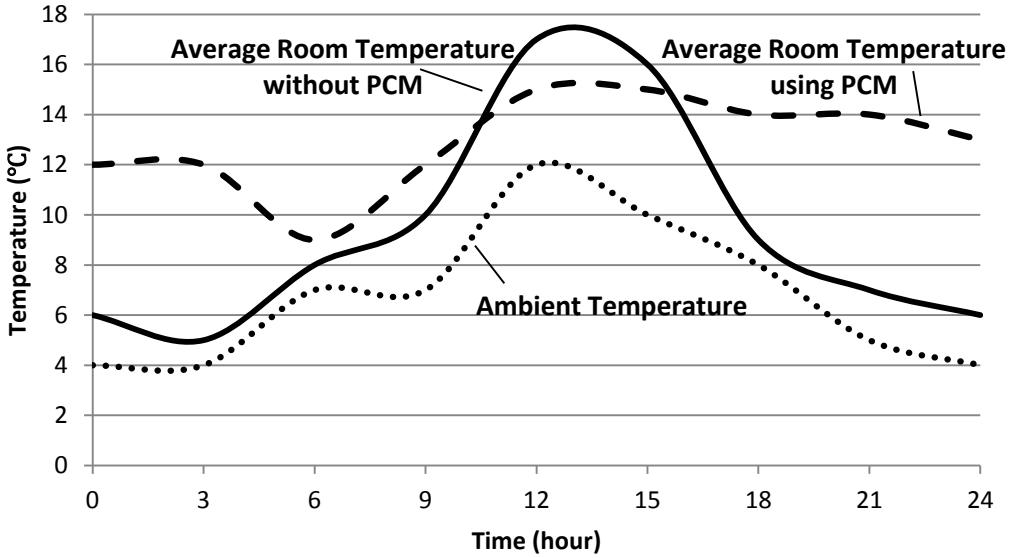

Fig. 12. Variation of average room temperature for a whole day

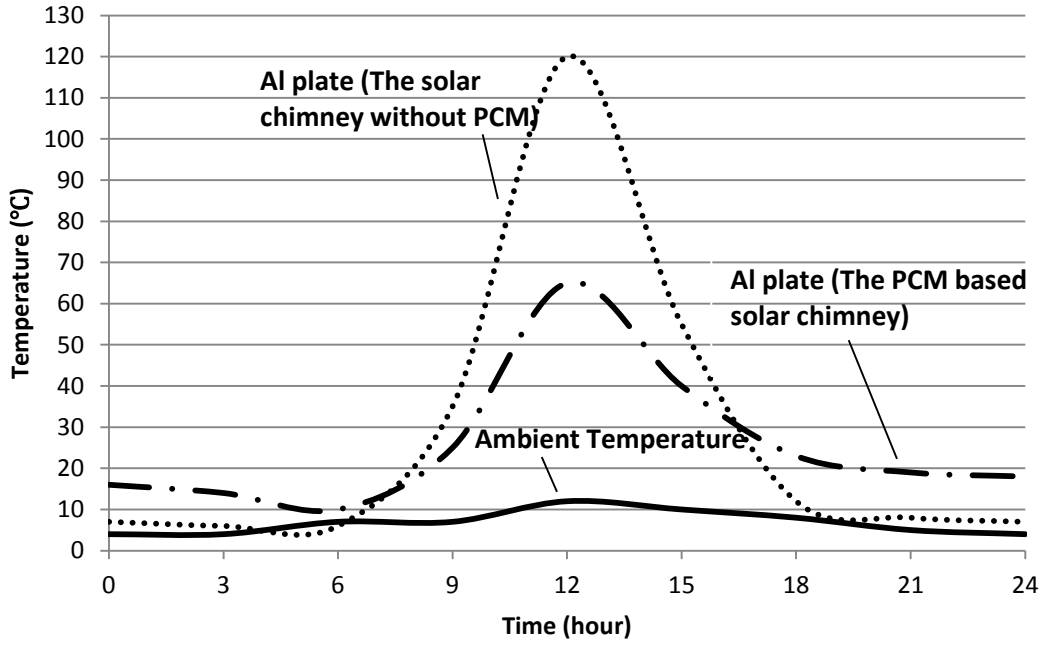

Fig. 13. Comparison of Al plate temperature between two different cases, the PCM-based solar chimney and without PCM

References

[1] Underwood C.P.: Modelling methods for energy in buildings, Thesis, School of the Built Environment, University of Northumbria at Newcastle.

[2] Chen H.Y., Riffat S.B., Zhu J.: Review of passive solar heating and cooling technologies, Renewable and Sustainable Energy Reviews, 14:781-89, 2010.

[3] Lee K.H., Strand R.K.: Enhancement of natural ventilation in buildings using a thermal chimney, Energy and Buildings; 41:615–21, 2009.

[4] Zhai X.Q., Song Z.P., Wang R.Z.: A review for the applications of solar chimneys in buildings, Renewable and Sustainable Energy Reviews, 15:3757–67, 2011.

[5] Gan G., Riffat S.B.: A numerical study of solar chimney for natural ventilation of buildings with heat recovery, Applied Thermal Engineering, 18(12):1171–87, 1998.

[6] Rodrigues A.M., Canha da Piedade A., Lahellec A., Grandpeix J.Y.: Modelling natural onvection in a heated vertical channel for room ventilation, Building and Environment, 35(5):455–69, 2000.

[7] Sharma A., Tyagi V., Chen C.R., Buddhi D., Review on thermal energy storage with phase change materials and applications, Renewable Sustainable Energy Reviews, 13(2):318–45, 2009.

[8] Li Y., Liu S.: Experimental study on thermal performance of a solar chimney combined with PCM, Applied Energy, 114:172-8, 2014.

[9] Voller V. R., Prakash C.: A Fixed-Grid Numerical Modelling Methodology for Convection-Diffusion Mushy Region Phase-Change Problems, Int. J. Heat Mass Transfer, 30:1709-1720, 1987.

[10] Duffie J.A., Beckman W.A.: Solar Energy Thermal Process, John Wiley and Sons Inc., 1974.

[11] Vahedi F.: Enhancing Thermal Efficiency of Double Skin Façade Buildings in Semi-Arid Climate, World Academy of Science, Engineering and Technology, Vol.7, 2013.